

Supplementary Information for

**DNA-nanohydrogel self-assembled gold nanoparticle: co-
profiling of multiple small molecule reductant in rat brain**

Jinpeng Mao, Shujun Wang, Wenliang Ji and Meining Zhang*

Department of Chemistry, Renmin University of China, Beijing, 100872, China.

** Email: mnzhang@ruc.edu.cn*

Experimental Procedures

Materials and Reagents. All the oligonucleotides were synthesized and purified by Sangon Biotechnology Co. Ltd (Shanghai, China), and their sequences are listed in Table S2. All the reagents were purchased from Sinopharm Chemical Reagent Co. Ltd. (Beijing, China). All chemicals were of reagent grade or better and used as received. All the oligonucleotides solution in this work was obtained by diluting the stock solution with a 20 mM Tris-HCl buffer (pH 7.4) which contained 140 mM NaCl and 5 mM KCl. The target small molecules were prepared with artificial cerebrospinal fluid (aCSF, pH 7.4). Artificial cerebrospinal fluid (aCSF) was prepared by dissolving NaCl (126 mM), KCl (2.4 mM), KH_2PO_4 (0.5 mM), MgCl_2 (0.85 mM), NaHCO_3 (27.5 mM), Na_2SO_4 (0.5 mM), and CaCl_2 (1.1 mM) into Millipore water.

Instrumentation. All the absorbance spectra were recorded using a Shimadzu 3600 UV-vis spectrophotometer (Shimadzu, Japan) at room temperature. Dynamic light scattering was conducted using a Zetasizer Nano ZS90 (Malvern, England). Water used throughout the experiments was purified by a Milli-Q system (Millipore, Bedford, MA, USA). Atomic force microscopic (AFM) measurements were carried out on a Bruker Nano Dimension Icon (Bruker, USA).

Animals. Adult male Sprague-Dawley rats (250–300 g) were purchased from Health Science Center, Peking University. The animals were housed on a 12:12 h light-dark schedule with free access to food and water. All animal procedures were approved by the Animal Care and Use Committee at National Center for Nanoscience and Technology of China and performed according to their guidelines. Animal handling was performed in accordance with local and international guidelines for use of laboratory animals. CSF and dialysate were achieved as our previous work.^{1,2}

Preparation of Gold Nanoparticle. The water-soluble AuNPs were synthesized according to the classical sodium citrate reduction method with a little adjustment.³ The 100 mL of 1 mM $\text{HAuCl}_4 \cdot 4\text{H}_2\text{O}$ solution was prepared in a three-necked flask and was heated to reflux for 5 minutes under vigorous stirring, then 10 mL of 38.8 mM sodium citrate solution was immediately added into the boiling solution with a color change from light yellow to wine red. After the mixture was allowed reflux for another 15 minutes, the heating was stopped, but stirring was continued. Then the solution was cooled to the room temperature, filtered through a 0.22 μm membrane filter and stored in a fridge of 4 °C before being used. The concentration of AuNPs was calculated based on an extinction coefficient of $2.7 \times 10^8 \text{ M}^{-1} \cdot \text{cm}^{-1}$ at 520 nm according to the Beer-Lambert Law. The size of the AuNPs was about 13 nm.²⁻⁴

Preparation of Building Units and DNA nanohydrogels. The DNA nanohydrogels were prepared according to the literature report.⁵ Stoichiometric quantities of the ssDNA strands were separately added to three tubes with a TM buffer (20 mM Tris, 10 mM MgCl_2 , pH 7.5). Then each mixture was heated to 95 °C for 10 min and cooled to room temperature over 4 h to form the desired building units. For preparation of DNA nanohydrogels, in a typical experiment, a stock solution of the building units was prepared, in which stoichiometric amounts of three building units were added in TM buffer. The molar ratio of Y-shaped monomer A (YMA) to linker is 1:1.5, and that of YMB to linker is 2:1. After 4 μM of YMA and 1 μM of YMB were mixed with 6.5 μM of DNA linker, the mixture was heated to 95 °C for 10 min and cooled to room temperature over 4 h to form the DNA nanohydrogels. The DNA nanohydrogels were then washed with Millipore water, precipitated by centrifugation, and stored at 4 °C for future use.⁵

Fabrication of the probe Gel@AuNPs. Typically, stoichiometric quantities of the fabricated DNA nanohydrogel was added to AuNPs solution (120 μL) and the solution was incubated for 1 hour at

room temperature. The prepared probe was used for sensing small molecules. In this study, Gel-1@AuNPs and Gel-2@AuNPs were utilized as two sensing elements. The size difference between Gel-1 and Gel-2 is caused by the ratio between Y-DNA 1 and Y-DNA 2. Lower Y-DNA 2 ratio induces bigger nanoparticle diameters because Y-DNA 2 serves to block the extension of the nanohydrogel. Gel-1 (20 nm) and Gel-2 (36 nm) was synthesized according to the reported literature via changing the ratio between Y-DNA 1 and Y-DNA 2 (ca. 1:3, 1:2). And the size was confirmed by the atomic force microscopic after statistics.

Characterization of the Gel@AuNPs. We used dynamic light scattering (DLS) and atomic force microscopy (AFM) to determine the average particle size and morphology of the prepared DNA nanohydrogels. DLS revealed that the initial hydrodynamic diameter of the resulting DNA hydrogel nanoparticles. The DNA nanohydrogels were found to have well-defined 3D spherical structures as shown in Fig. S1. After the AuNPs were functionalized with the DNA nanohydrogel, the characteristic peak of Gel at 260 nm was significantly increased (Fig. S2a). What's more, the dynamic light scattering (DLS) experiments showed that the average hydrodynamic size increased about 12 nm (Fig. S2b) after DNA nanohydrogel decorated to the AuNPs. These results further confirming that the AuNPs were successfully assembled with the DNA nanohydrogel.

Determination GSH using the Gel@AuNPs. In the GSH detection step, the Gel@AuNPs was incubated with GSH of a series of concentration in aCSF. UV-vis absorbance measurements were thereafter performed after another 30 minutes incubation and every experiment was performed in triplicate. Only difference between the sensing assay is the concentration of GSH. Firstly, we evaluated the response of Gel@AuNPs to other small molecules in artificial cerebrospinal fluid. Satisfactory response signal of the Gel@AuNPs for GSH analysis was achieved as shown in Fig. S3 though it was not a specific recognition process (the response signal of GSH was obviously higher than other molecules even at a lower concentration). Then, the feasibility of proposed Gel@AuNPs for GSH detection in aCSF was investigated as shown in Fig. S4. As shown, the linear range was determined to be from 40 nM to 100 μ M. The linear equation is $(A-A_0)/A_0 = 0.111\lg C + 0.180$ with a limit of detection (LOD) of 40 nM. This result demonstrated that the proposed Gel@AuNPs for GSH detection in aCSF exhibits good sensitivity. We further investigated the validity of Ge@AuNPs for GSH detection in the dialyzate. After achieving the absorbance spectrum of designed Gel@AuNPs in the dialyzate of rat brain. According to the linear equation achieved in the aCSF system using the designed Gel@AuNPs, the GSH concentration in dialyzate was calculated to be ca. 13 μ M (n=4).

Discrimination of ten small molecules. The as-prepared Gel@AuNPs were employed to this multidimensional sensor for the detection of small molecules. The stoichiometric quantities of molecule solution or blank solution was mixed with as-prepared Gel-1@AuNPs and Gel-2@AuNPs solution and incubated for about 30 minutes at room temperature. Then, the mixture was diluted and the absorbance of the mixture at 520 nm and 620 nm were recorded. Taking Gel-1@AuNPs as an example, the absorbance spectra of the Gel-1@AuNPs in aCSF containing different small molecules are shown in Fig.S8. The changes in the two optical signals of Gel-1@AuNPs and Gel-2@AuNPs lead to the discrimination of small molecules.

Stability of the Gel@AuNPs. The stability of the Gel@AuNPs was evaluated through kinetic UV-vis spectra. As shown in Fig S9a, kinetics of the bare Gel@AuNPs were monitored by an absorbance spectrum in the visible region every 30 minutes. The absorbance spectra of Gel@AuNPs are very stable. DLS was also applied to demonstrate the stability of Gel@AuNPs. As shown in Fig. S9b,

there is no obvious size change for the assembled Gel@AuNPs every one day, which indicating the stability of the Gel@AuNPs. To confirm that the collapse of DNA nanohydrogel was ascribed to the addition of small molecule reductants. Kinetic UV-vis spectra were also conducted. The ratio of A_{620}/A_{520} increased after the addition of GSH as shown in Fig. S9c. The enhancement was fast in the first 3-5 min, turned slowly, then levelled off after about 12 min. This change in ratio of A_{620}/A_{520} after the addition of GSH is a typical interaction kinetics process.

Data analysis. All measurements were repeated to generate six replicates for each molecule. The data was analyzed by the linear discriminant analysis (LDA) applying Mahalanobis clustering analysis and hierarchical cluster analysis (HCA). LDA is a type of statistic software to recognize the linear combination of features that differentiate two or more classes of object or event, which can transform the raw response patterns to canonical patterns, and maximizes the ratio of between-class variance to within-class variance, thereby it can enable maximal separability according to the preassigned grouping. HCA is a model-free method based on the grouping of the analyte vectors according to their spatial distances in their full vector space. After the analysis, two canonical factors were generated that represented linear combinations of the response matrices, obtained from the absorbance response patterns (two channels \times ten small molecules \times six replicates). The two significant discrimination factors were used to generate a two plot.^{4,6,7}

Disulfide linkage converted to the sulfhydryl group. To confirm disulfide linkage (-S-S) in the DNA nanohydrogel was translated into -SH, experiment was conducted as following. There is no absorption peak for 5,5'-dithiobis-2-nitrobenzoic acid (DTNB) at about 412 nm. When it reacted with compounds with -SH, 2-nitro-5-mercaptobenzoic acid (TNB²⁻) was formed according to the literature report as shown in Fig. S10a. The product TNB²⁻ has a strong absorption peak at 412nm. In order to eliminate interruptions from small molecule contain -SH (e.g. GSH, Cys and H₂S), we selected small molecule reductant AA as a target. The DTNB was dissolved in 0.1M phosphate buffer solution (pH=8.0) contain 1.0 mM EDTA. As shown in the Fig. S10b, there is no obvious absorption peak at 412 nm for the sample bare DTNB (black line) and DTNB contained DNA nanohydrogel (red line). In the presence of 0.1 μ M AA, the DNA nanohydrogel was collapsed. The collapsed DNA nanohydrogel was then mixing with the DTNB. The collapsed gel was reacted with DTNB for 15 min before record the absorbance spectra. As except, the DTNB was transformed into TNB²⁻, the solution color turned to faint yellow, a significant absorption peak was observed at 412 nm. Indicating the -S-S-linkage was translated into -SH.^{8,9}

Equilibrium among AuNPs, DNA nanohydrogel and small molecules. The biggest difference between the five groups in LDA of the ten small molecules is their reducing capacities of these small molecules. Firstly, small molecules with sulfydryl (e.g. GSH, H₂S and Cys) would react with disulfide linkages in the DNA nanohydrogel easily by classical sulfhydryl-disulfhydryl exchange reaction. This reaction contributes to the strong response to the GSH react with Gel@AuNPs. Secondly, the bare AuNPs or Gel@AuNPs is negatively charged, the pH value of the probe solution (aCSF) was about 7.4. It means the reducing substances with lower pI could be negatively charged, which could not bind to the Gel@AuNPs more effectively, result in the protection of DNA nanohydrogels receptors. Thirdly, sulfydryl (-SH) exhibited much stronger reducing capacity than hydroxy (-OH), thus small molecule reductants with sulfydryl (GSH, H₂S and Cys) show stronger reducing capacity than those with hydroxy (DA, DOPAC, 5-HT, Ne, AA and Glu), which facilitate the reduction of disulfide bonds in the building units of DNA nanohydrogel. It is notably that small molecule reductants with more than two hydroxy while no sulfydryl (DA, DOPAC, Ne and AA)

will be more unstable when subjected to oxygen when conducting in vitro experiment, especially AA with four hydroxy. The inevitable oxidation of these substances makes them lose or greatly restrains their reducing capacities. Moreover, as the two DNA nanohydrogel receptors have different size, then the protection capacity of AuNPs from aggregation are different, leading to the different response to reducing substances by various interactions such as electrostatic interaction or hydrogen bonding. Furthermore, some reducing substance without reducing ability could protect the AuNPs from aggregation too. As a result, we attribute the final response signal to the equilibrium among AuNPs, DNA nanohydrogel and small molecule reductants.

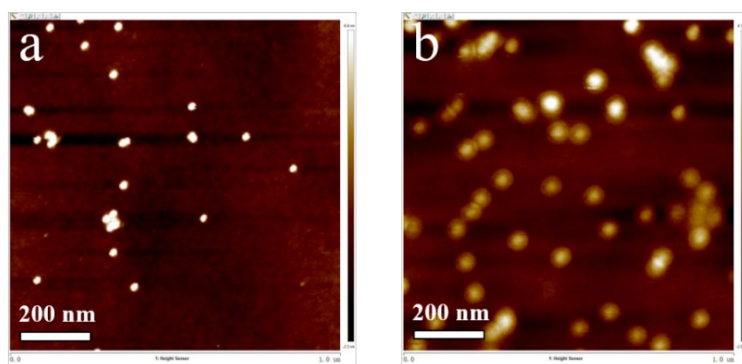


Fig. S1 AFM images of the (a) DNA nanohydrogel, (b) DNA nanohydrogel modified AuNPs.

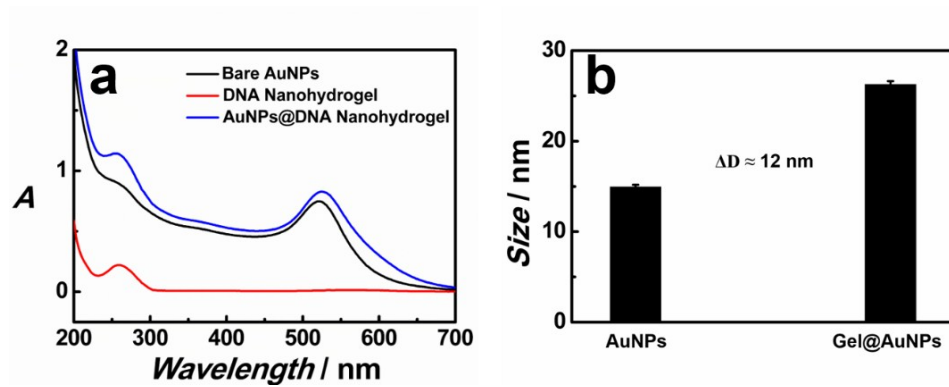


Fig. S2 (a) UV-vis spectra of bare AuNPs, DNA nanohydrogel and the developed Gel@AuNPs probe in H₂O. (b) Hydrodynamic diameter distribution determined by dynamic light scattering in H₂O.

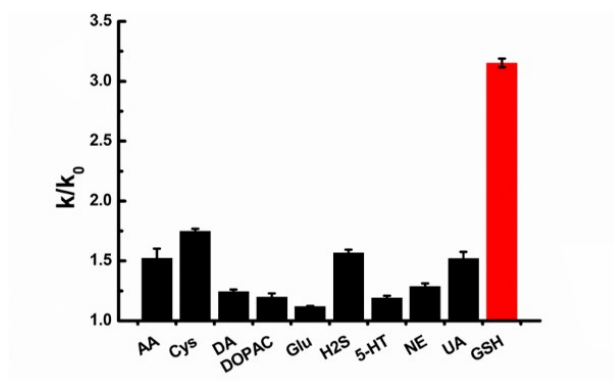


Fig. S3 The absorbance ratio k/k_0 of the Gel@AuNPs in the mixture solution (aCSF) containing the target GSH (1 μM) and other non-target small molecules (5 μM).

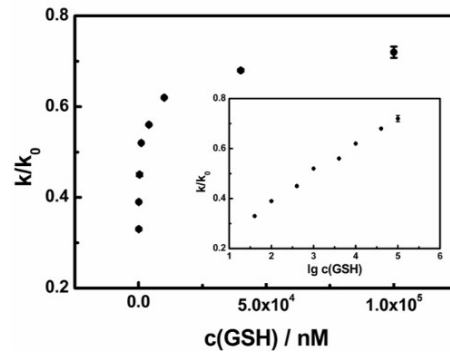


Fig. S4 The absorbance spectra of the Gel@AuNPs in the mixture solution (aCSF) containing different concentrations of GSH;

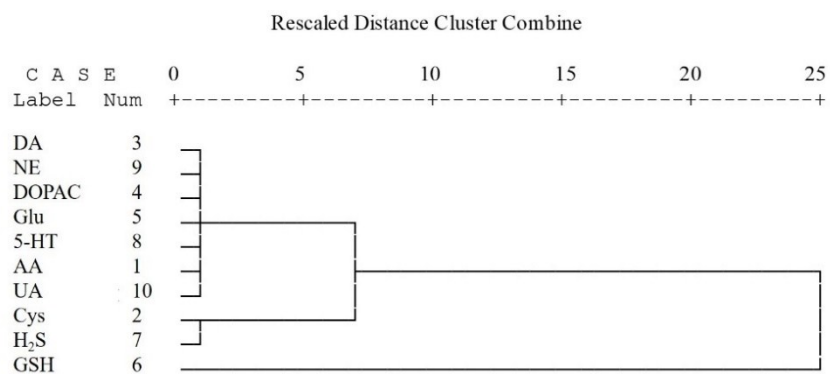


Fig. S5 Hierarchical cluster analysis dendrogram for ten small molecules analytes at 1 μ M, all experiments were run in six replicates.

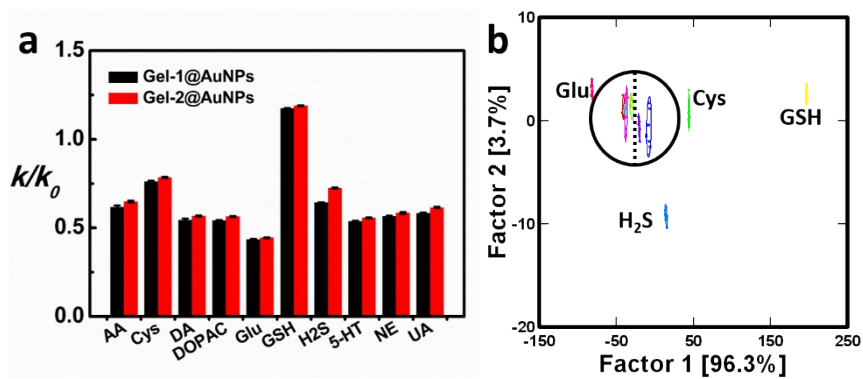


Fig. S6 Pattern recognition of small molecules at 1 μ M in the presence of additional cerebrospinal fluid. a) fingerprints and b) canonical score plot for the response patterns as obtained from LDA for ten selected neurochemicals at 1 μ M.

Gel-1@AuNPs	Gel-2@AuNPs	Correct / %
		83%
		67%
		100%

Fig. S7 Jackknifed classification matrix obtained using LDA of two sensing channels for ten small molecules.

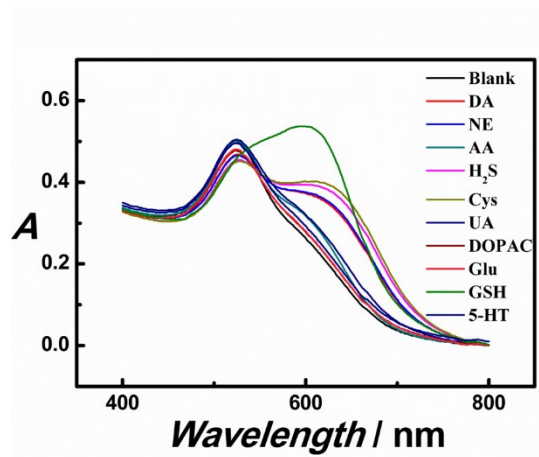


Fig. S8 The absorbance spectra of the Gel-1@AuNPs in aCSF containing different small molecules (0.1 mM).

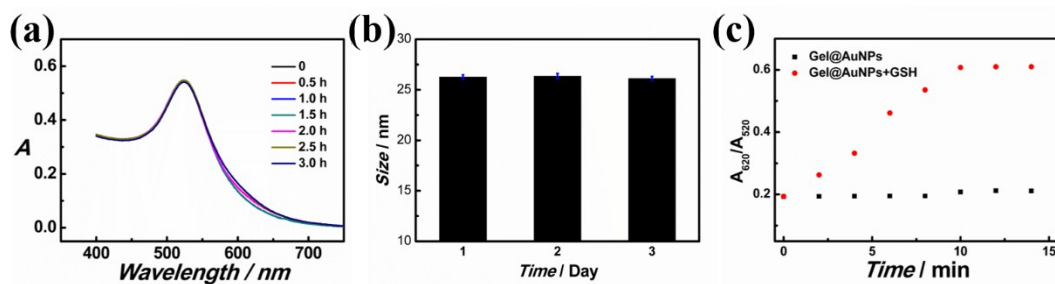


Fig. S9 (a) Kinetic UV-vis spectra of the Gel-1@AuNPs monitored by an absorbance spectrum in the visible region every 30 minutes. (b) Hydrodynamic diameter distribution determined by dynamic light scattering in H₂O of Gel@AuNPs every one day. (c) Kinetic UV-vis spectra of the Gel-1@AuNPs before and after the addition of 0.1 μM GSH.

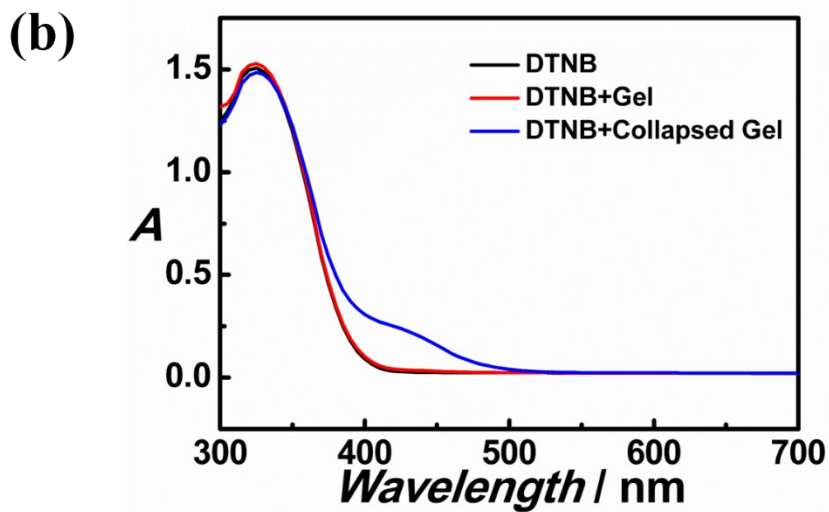
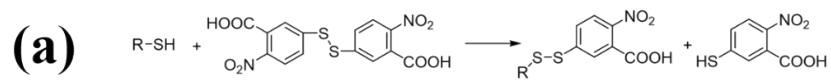


Fig. S10 a) Schematic illustration of the reaction of DTNB and -SH. b) The absorbance spectra of bare DTNB (black line), DTNB containing DNA nanohydrogel (red line) and DTNB in the presence of collapsed DNA nanohydrogel (blue line).

Table S1. Selected ten small molecules and their abbreviations

Analytes	MW/(g/mol)	pI	Purity
Ascorbic Acid (AA)	176.12	--	>98%
Cysteine (Cys)	121.15	5.05	>98%
Dopamine (DA)	189.64	--	>98%
Dihydroxyphenylacetic Acid (DOPAC)	168.15	--	>95%
Glutamic Acid (Glu)	147.13	3.22	>98%
Glutathione (GSH)	307.32	5.93	>98%
Sulfuretted Hydrogen (H ₂ S)	240.18	--	>98%
5-hydroxytryptamine (5-HT)	212.68	--	>98%
Noradrenaline (NE)	169.18	--	>95%
Uric Acid (UA)	168.11	--	>95%

All the reagents were purchased from Sinopharm Chemical Reagent Co. Ltd. (Beijing, China).

Table S2. List of DNA sequences used in the study

Building units	Name	Detailed sequence information
YMA	A1	GAG GCG CCC AGG CTA GCT ACA ACG ACT CCG CCG CCC GAA ATC AGC TTC T
	A2	AAC ATA GTA GTT AGT TGT AGC TAG C(S-S) CT GGG CGC CTC GAA ATC AGC TTC T
	A3	GGG CCG CG(S-S)G AGT CGT ACT AAC TAC TAT GTT GAA ATC AGC TTC T
YMB	B1	AAC ATA GTA GTT AGT TGT AGC TAG CCT GGG
	B2	GGG CCG CGG AGT CGT ACT AAC TAC TAT GTT
Linkers	linker 1	GTC CCG CCT GTG ACA TGC ATT AGA AGC TGA TTT C
	linker 2	AAT GCA TGT CA(S-S)C AGG CGG GAC AGA AGC TGA TTT C

Table S3. Training matrix of the response patterns against various small molecules at 1 μ M in aCSF

Molecules	Gel-1@AuNPs	Gel-2@AuNPs
AA	1.263	1.428
AA	1.258	1.452
AA	1.247	1.414
AA	1.243	1.408
AA	1.279	1.443
AA	1.265	1.451
Cys	2.052	2.500
Cys	2.053	2.500
Cys	2.062	2.491
Cys	2.054	2.516
Cys	2.054	2.525
Cys	2.064	2.524
DA	1.101	1.182
DA	1.093	1.164
DA	1.108	1.166
DA	1.119	1.221
DA	1.103	1.198
DA	1.104	1.194
DOPAC	1.073	1.115
DOPAC	1.067	1.123
DOPAC	1.075	1.113
DOPAC	1.087	1.119
DOPAC	1.083	1.105
DOPAC	1.079	1.115
Glu	1.006	1.004
Glu	1.004	1.000
Glu	1.003	1.024
Glu	0.993	0.997
Glu	0.996	1.009
Glu	1.003	1.000
GSH	2.999	3.951
GSH	2.997	3.929
GSH	2.997	3.950
GSH	3.009	3.906
GSH	3.002	3.932
GSH	3.012	3.937
H ₂ S	1.995	2.357
H ₂ S	1.999	2.360
H ₂ S	1.995	2.361
H ₂ S	2.019	2.368

H ₂ S	1.999	2.346
H ₂ S	2.000	2.348
5-HT	1.051	1.041
5-HT	1.043	1.049
5-HT	1.044	1.069
5-HT	1.062	1.058
5-HT	1.050	1.055
5-HT	1.031	1.043
NE	1.150	1.215
NE	1.144	1.199
NE	1.161	1.193
NE	1.158	1.221
NE	1.155	1.224
NE	1.172	1.187
UA	1.207	1.331
UA	1.207	1.318
UA	1.203	1.320
UA	1.211	1.324
UA	1.212	1.336
UA	1.225	1.336

Table S4. Training matrix of the response patterns against various small molecules at 1 μ M in CSF

Molecules	Gel-1@AuNPs	Gel-1@AuNPs
AA	0.617	0.647
AA	0.629	0.647
AA	0.614	0.656
AA	0.613	0.652
AA	0.627	0.648
AA	0.605	0.641
Cys	0.757	0.785
Cys	0.757	0.784
Cys	0.770	0.781
Cys	0.762	0.788
Cys	0.760	0.784
Cys	0.763	0.786
DA	0.543	0.568
DA	0.533	0.569
DA	0.537	0.569
DA	0.555	0.569
DA	0.544	0.566
DA	0.549	0.561
DOPAC	0.542	0.562
DOPAC	0.542	0.561
DOPAC	0.541	0.564
DOPAC	0.544	0.567
DOPAC	0.541	0.564
DOPAC	0.546	0.566
Glu	0.435	0.442
Glu	0.435	0.445
Glu	0.432	0.444
Glu	0.439	0.442
Glu	0.435	0.449
Glu	0.437	0.444
GSH	1.176	1.191
GSH	1.173	1.188
GSH	1.178	1.188
GSH	1.172	1.190
GSH	1.172	1.192
GSH	1.169	1.188
H ₂ S	0.640	0.724
H ₂ S	0.642	0.730
H ₂ S	0.641	0.722
H ₂ S	0.645	0.722
H ₂ S	0.643	0.721

H ₂ S	0.646	0.728
5-HT	0.540	0.558
5-HT	0.537	0.556
5-HT	0.531	0.554
5-HT	0.536	0.560
5-HT	0.535	0.556
5-HT	0.541	0.554
NE	0.561	0.580
NE	0.563	0.589
NE	0.570	0.590
NE	0.568	0.584
NE	0.563	0.581
NE	0.567	0.581
UA	0.587	0.615
UA	0.583	0.613
UA	0.586	0.611
UA	0.582	0.615
UA	0.580	0.619
UA	0.585	0.617

Table S5. Identification of unknown small molecules samples at 1 μM in aCSF using the Gel@AuNPs.

	Gel-1@AuNPs	Gel-2@AuNPs	Identification	Verification
1	1.044	1.119	DOPAC	DOPAC
2	2.001	2.516	Cys	Cys
3	2.002	2.361	H ₂ S	H ₂ S
4	1.267	1.406	AA	AA
5	1.039	1.062	5-HT	5-HT
6	1.024	0.968	Glu	Glu
7	1.211	1.331	UA	UA
8	1.144	1.192	NE	NE
9	1.283	1.401	AA	AA
10	2.996	3.952	GSH	GSH
11	1.998	2.345	H ₂ S	H ₂ S
12	1.117	1.218	DA	DA
13	1.263	1.406	AA	AA
14	1.159	1.221	NE	NE
15	1.221	1.335	UA	UA
16	3.000	3.934	GSH	GSH
17	2.038	2.500	Cys	Cys
18	1.050	1.115	DOPAC	DOPAC
19	1.199	1.334	UA	UA
20	1.999	2.359	H ₂ S	H ₂ S
21	1.210	1.328	UA	UA
22	1.162	1.199	NE	NE
23	1.998	2.500	Cys	Cys
24	1.278	1.394	AA	AA
25	1.103	1.192	DA	DA
26	0.997	0.964	Glu	Glu
27	1.034	1.054	5-HT	5-HT
28	1.151	1.190	NE	NE
29	1.043	1.053	5-HT	5-HT
30	2.998	3.947	GSH	GSH
31	1.109	1.214	DA	DA
32	1.999	2.491	Cys	Cys
33	1.105	1.231	DA	DA
34	1.051	1.115	DOPAC	DOPAC
35	1.062	1.105	DOPAC	DOPAC
36	2.999	3.941	GSH	GSH
37	1.051	1.064	5-HT	5-HT
38	1.995	2.360	H ₂ S	H ₂ S
39	1.000	0.972	Glu	Glu
40	1.000	0.968	Glu	Glu

Table S6. Identification of unknown small molecules samples at 1 μ M in CSF

	Gel-1@AuNPs	Gel-2@AuNPs	Identification	Verification
1	0.581	0.618	UA	UA
2	0.537	0.556	5-HT	5-HT
3	1.173	1.188	GSH	GSH
4	0.542	0.564	DOPAC	DOPAC
5	0.623	0.646	AA	AA
6	0.551	0.569	DA	DA
7	0.642	0.729	H2S	H2S
8	0.584	0.613	UA	UA
9	0.534	0.557	5-HT	5-HT
10	0.438	0.446	Glu	Glu
11	0.645	0.729	H2S	H2S
12	0.754	0.779	Cys	Cys
13	0.621	0.646	AA	AA
14	1.171	1.187	GSH	GSH
15	0.568	0.582	NE	NE
16	0.585	0.615	UA	UA
17	0.544	0.563	DOPAC	DOPAC
18	0.545	0.568	DA	DA
19	0.434	0.448	Glu	Glu
20	0.541	0.563	DOPAC	DOPAC
21	0.553	0.565	DA	DA
22	0.615	0.652	AA	AA
23	0.766	0.786	Cys	Cys
24	1.169	1.188	GSH	GSH
25	0.569	0.587	NE	NE
26	0.583	0.619	UA	UA
27	0.534	0.558	5-HT	5-HT
28	0.567	0.584	NE	NE
29	1.174	1.188	GSH	GSH
30	0.437	0.442	Glu	Glu
31	0.619	0.651	AA	AA
32	0.758	0.789	Cys	Cys
33	0.549	0.567	DOPAC	DA
34	0.645	0.724	H2S	H2S
35	0.561	0.586	NE	NE
36	0.64	0.728	H2S	H2S
37	0.431	0.446	Glu	Glu
38	0.761	0.781	Cys	Cys
39	0.558	0.567	DA	DOPAC
40	0.536	0.555	5-HT	5-HT

References

1. S. Wang, X. Liu, and M. Zhang, *Anal. Chem.*, 2017, **89**, 5382–5388.
2. J. Mao, M. Xu, W. Ji and M. Zhang, *Chem. Commun.*, 2018, **54**, 1193-1196.
3. J. Liu and Y. Lu, *Nat Protoc*, 2006, **1**, 246-252.
4. W. Sun, Y. Lu, J. Mao, N. Chang, J. Yang and Y. Liu, *Anal. Chem.*, 2015, **87**, 3354–3359.
5. J. Li, C. Zheng, S. Cansiz, C. Wu, J. Xu, C. Cui, Y. Liu, W. Hou, Y. Wang, L. Zhang, I. T. Teng, H. H. Yang and W. Tan, *J. Am. Chem. Soc.*, 2015, **137**, 1412-1415.
6. P. C. Jurs, G. A. Bakken and H. E. McClelland, *Chem. Rev.*, 2000, **100**, 2649-2678.
7. A. Bajaj, O. R. Miranda, R. Phillips, I.-B. Kim, D. J. Jerry, U. H. F. Bunz and V. M. Rotello, *J. Am. Chem. Soc.*, 2010, **132**, 1018-1022.
8. P. W. Riddles, R. L. Blakeley, B. Zerner, *Anal. Biochem.*, 1979, **94**, 75–81.
9. T. W. Thannhauser, Y. Konishi, H. A. Scheraga, *Anal. Biochem.*, 1984, **138**, 181-188.